

Propagation of a Strong Fast Magnetosonic Wave in the Magnetosphere of a Neutron Star

ALEXANDER Y. CHEN,¹ YAJIE YUAN,¹ XINYU LI,² AND JENS F. MAHLMANN³

¹*Physics Department and McDonnell Center for the Space Sciences, Washington University in St. Louis, MO, 63130, USA*

²*Canadian Institute for Theoretical Astrophysics, 60 St George St, Toronto, ON M5R 2M8*

³*Department of Astrophysical Sciences, Princeton University, Princeton, NJ 08544, USA*

ABSTRACT

We study the propagation of a strong, low frequency, linearly polarized fast magnetosonic wave inside the magnetosphere of a neutron star. The relative strength $\delta B/B$ of the wave grows as a function of radius before it reaches the light cylinder, and what starts as a small perturbation can grow to become nonlinear before it escapes the magnetosphere. Using first-principles Particle-in-Cell (PIC) simulations, we study in detail the evolution of the wave as it becomes nonlinear. We find that an initially sinusoidal wave becomes strongly distorted as $\delta B/B$ approaches order unity. The wave steepens into a shock in each wavelength. The plasma particles drift into the shock and undergo coherent gyration in the rest of the wave, and subsequently become thermalized. This process quickly dissipates the energy of an FRB emitted deep within the magnetosphere of magnetar, effectively preventing GHz waves produced in the closed field line zone from escaping. This mechanism may also provide an effective way to launch shocks in the magnetosphere from kHz fast magnetosonic waves without requiring a relativistic ejecta. The resulting shock can propagate to large distances and may produce FRBs as a synchrotron maser.

Keywords: magnetic fields — plasma physics — relativistic processes — shock waves — stars: neutron

1. INTRODUCTION

Neutron stars are capable of producing low frequency fast magnetosonic (fms) waves from within the magnetosphere. Star quakes in the crust can launch Alfvén waves along the magnetic field (e.g. Bransgrove et al. 2020), which can convert spontaneously to fms waves due to propagation on curved field lines (Yuan et al. 2021). These waves have a low characteristic frequency of $\omega \sim 10$ kHz (Blaes et al. 1989), much lower than the plasma and gyro-frequencies within the magnetosphere.

Fast radio bursts (FRBs), in some theoretical models, are also believed to originate from within the magnetosphere of neutron stars (in particular magnetars) initially as fast magnetosonic waves. These bursts are short, millisecond duration signals in the MHz to GHz radio frequencies (see e.g. Petroff et al. 2019 for a review), and recent observations of a simultaneous FRB and an X-ray burst from a galactic magnetar SGR 1935+2154 have corroborated the association of FRBs with strongly magnetized neutron stars (see e.g. CHIME/FRB Collaboration et al. 2020; Bochenek et al. 2020; Mereghetti et al. 2020). Two broad classes of theoretical models for FRBs exist. One invokes a

shock produced by a relativistic ejecta in the wind at large distances, and both theory and simulations have shown that the shock front is capable of generating coherent GHz emission through the synchrotron maser mechanism (Lyubarsky 2014; Plotnikov & Sironi 2019; Sironi et al. 2021). The other class of models invoke plasma instabilities close to the magnetar, either creating “bunches” of charged particles which radiate coherently (Kumar et al. 2017; Lu et al. 2020) or producing GHz waves in reconnecting current sheets (Lyubarsky 2020). If the FRB is produced close enough to the star, then its frequency may be lower than the local plasma and gyro-frequencies, and its behavior will be similar to the low frequency fms waves produced by star quakes.

As these low frequency fms waves propagate outwards, they may become nonlinear ($\delta B \gtrsim B_{\text{bg}}$), and it was recently proposed that these waves may suffer very strong scattering (Beloborodov 2022, 2021) by charged particles in the magnetosphere, depending on their propagation angle with respect to the background magnetic field (Qu et al. 2022). However, this scenario was studied only considering the response of a single test particle. If the wave becomes nonlinear while collective plasma effects are important (e.g. when plasma frequency exceeds the wave frequency, $\omega_p > \omega$), then the plasma response may significantly alter the wave itself, potentially leading to a completely different dissipation mechanism. In this paper, we use first-principles Particle-in-Cell (PIC) sim-

ulations to study the evolution of the low frequency fms wave as it becomes nonlinear in a dense plasma. We will consider both \sim kHz waves produced by seismic activity on the star, as well as an FRB produced deep within the magnetosphere. We will discuss how the results apply to each case, and potential observational implications.

2. PROPAGATION OF FAST MAGNETOSONIC WAVES

The highly magnetized surroundings of a magnetar is often considered to be approximately “force-free”, where the plasma inertia is negligible compared to the magnetic field energy density. This is the limit of magneto-hydrodynamics (MHD) where the electromagnetic force on the plasma is zero, $\rho\mathbf{E} + \mathbf{j} \times \mathbf{B} = 0$. Two assumptions are required for the force-free approximation: $\mathbf{E} \cdot \mathbf{B} = 0$, and $E < B$. Under this approximation, MHD waves simplify to only two modes: the Alfvén mode, which has its electric field vector $\delta\mathbf{E}$ in the plane of the wave vector \mathbf{k} and the background magnetic field \mathbf{B}_{bg} ; and the fast magnetosonic (fms) mode, which has $\delta\mathbf{E}$ perpendicular to the \mathbf{k} - \mathbf{B}_{bg} plane (see e.g. Arons & Barnard 1986). The Alfvén mode propagates along the background magnetic field, while only the fms mode can propagate freely across the field lines and escape the magnetosphere. Therefore, in this paper, we only consider fast modes that are produced in the closed zone and propagate quasi-perpendicularly to the background magnetic field.

In the closed zone of the neutron star, where the background magnetic field scales as $B_{\text{bg}} \sim r^{-3}$, the amplitude of the fast wave scales as $\delta B \sim r^{-1}$ since it expands spherically from the emission site. Therefore, the relative amplitude of the wave increases rapidly as $\delta B/B_{\text{bg}} \sim r^2$. Consider a cosmological FRB produced deep within the magnetosphere as a coherent fms wave. Its luminosity determines the radius r_{NL} where its amplitude becomes comparable to the background magnetic field:

$$r_{\text{NL}} \sim \sqrt{B_0 r_*^3} \left(\frac{L}{c}\right)^{-1/4} \sim 1.3 \times 10^8 B_{0,14}^{1/2} L_{42}^{-1/4} \text{ cm} \quad (1)$$

For all known magnetars, this is far within the light cylinder, $r_{\text{NL}} \ll r_{\text{LC}}$. Take the galactic magnetar SGR 1935+2154 as an example: its spin period is $P \approx 3.2$ s and its spindown magnetic field is $B_0 \sim 2 \times 10^{14}$ G. An FRB of isotropic equivalent luminosity $L \gtrsim 2 \times 10^{34}$ erg/s will have a nonlinear radius r_{NL} within the light cylinder. The two consecutive radio bursts observed in 2020 satisfy this criterion since they have isotropic luminosities of order $L \sim 10^{37}$ erg/s (CHIME/FRB Collaboration et al. 2020).

Consider the simplified case where the wave propagates perpendicularly to the background field \mathbf{B}_{bg} . The wave magnetic field $\delta\mathbf{B}$ is perpendicular to the wave vector \mathbf{k} and the wave electric field $\delta\mathbf{E}$, therefore it lies along the background magnetic field. When

$\delta B/B_{\text{bg}} > 1/2$, the combined magnetic field B_{tot} may become smaller than the wave electric field. This can potentially create local $E > B$ regions which breaks ideal MHD, which is also the basis of the force-free approximation. If the plasma remains well magnetized, $\omega_B \gg \omega_p \gg \omega$, then its response may prevent such $E > B$ regions to develop in the first place. The plasma response involves its inertia in nature and cannot be probed through force-free calculations. In a typical force free simulation, in order to preserve the force-free condition, any $E > B$ is brought to $E = B$, resulting in artificial dissipation (e.g. Li et al. 2019).

Whether plasma remains well magnetized at the nonlinear radius r_{NL} depends on its density distribution over radius $n_{\pm}(r)$. Magnetars are known to emit X-rays that are often more luminous than their spindown power, therefore some form of magnetic dissipation is in general believed to occur in the magnetosphere (e.g. Thompson & Duncan 1996). As a side effect of the magnetic dissipation, a much higher pair multiplicity is expected compared to ordinary pulsars. Beloborodov (2021) estimated the pair density in the magnetospheres of magnetars using their typical X-ray luminosity:

$$n_{\pm}(r) \sim 10^{10} r_9^{-3} \left(\frac{L_{\text{keV}}}{10^{35} \text{ erg/s}}\right) \text{ cm}^{-3}. \quad (2)$$

We can use this to estimate the gyrofrequency and plasma frequency at the nonlinear radius r_{NL} :

$$\omega_B(r_{\text{NL}}) \sim 8.0 \times 10^{14} B_{0,14}^{-1/2} L_{\text{wave},42}^{3/4} \text{ Hz}, \quad (3)$$

$$\omega_p(r_{\text{NL}}) \sim 1.2 \times 10^{11} B_{0,14}^{-3/4} L_{\text{wave},42}^{3/8} L_{\text{keV},35}^{1/2} \text{ Hz}. \quad (4)$$

Both frequencies are much higher than the typical GHz frequency seen in FRBs and satisfy $\omega_B \gg \omega_p \gg \omega$, hence we expect that the plasma should remain in the MHD regime and exhibit collective behavior in response to potential $E > B$ regions in the wave.

The propagation of a fast wave in a constant background magnetic field where $\delta B/B_{\text{bg}}$ is close to 1/2 was studied by Lyubarsky (2003). The wave eventually steepens into a shock due to nonlinearity, and he calculated the time scale for shock formation in the MHD framework. For intermediate wave amplitudes $\delta B < B_{\text{bg}}/2$, the shock formation time is $t \sim \sigma/\omega$, where σ is the plasma magnetization and ω is the wave frequency, while this time decreases to zero when the wave amplitude approaches $B_{\text{bg}}/2$.

In the case of a decreasing background magnetic field however, this calculation may not apply directly. If B_{bg} varies quickly enough, the wave may not have enough time to steepen, and $E > B$ regions may be forced to develop. As a result, plasma may be accelerated in these regions and become demagnetized, at which point MHD assumptions no longer hold. On the other hand, if B_{bg} varies relatively slowly, but faster than the shock formation time at constant background field, then the

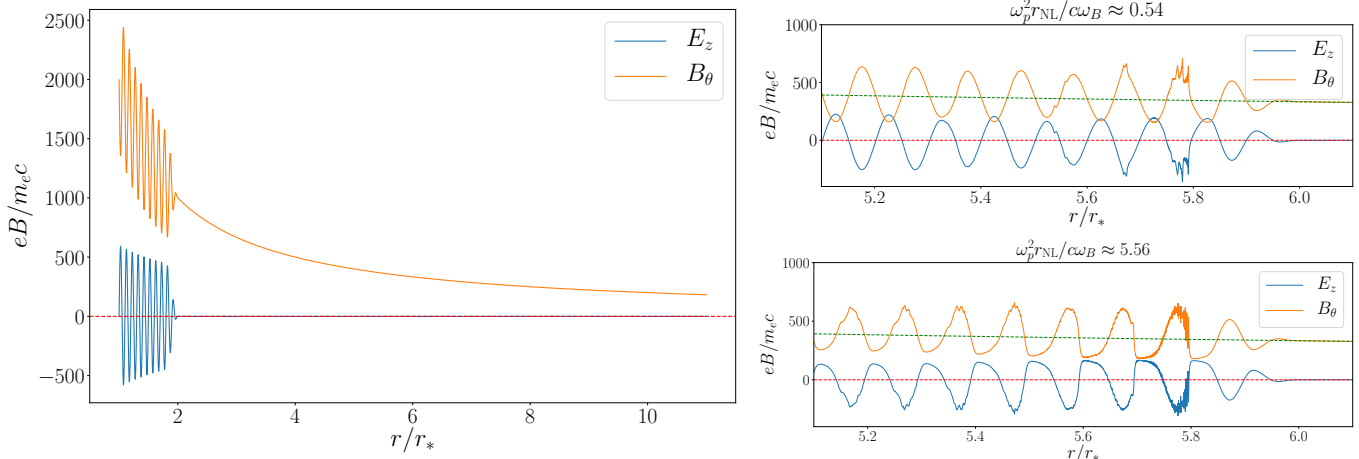


Figure 1. *Left:* Snapshot of the early stage of a simulation at $t \approx r_*/c$, where a wave is launched from $r = r_*$, before it becomes nonlinear near $r_{\text{NL}} \approx 2.7r_*$. *Right:* Snapshot of two simulations at $t \approx 5r_*/c$. The only difference between the two runs is ω_p . The bottom run clearly shows the development of a shock in the leading wavelength, while the top run develops $E > B$ regions. Dashed lines in the right panel show the background fields B_{bg} (green) and E_{bg} (red).

wave may steepen much faster due to $\delta B/B_{\text{bg}}$ quickly approaching $1/2$, reducing the timescale for shock development. In the following sections, we will use direct PIC simulations to study the evolution of a fms wave traveling across a decreasing background magnetic field. Our goal is to derive a more appropriate criterion for shock development, and estimate the dissipation power resulting from this process.

3. NUMERICAL SIMULATIONS

3.1. Setup

To simplify the problem into a quasi-1D one, we substitute the magnetosphere of a neutron star with that of an infinitely long cylinder of radius r_* carrying a uniform current along z direction. It is surrounded by a toroidal magnetic field $B_{\theta, \text{bg}} = B_0(r/r_*)^{-1}$. We launch a fast wave from the surface of the cylinder with initial amplitude $\delta B_0 \ll B_0$ and polarization δE along z , such that the wave propagates outwards along the radial direction \hat{r} , and the wave magnetic field δB is along the background magnetic field. As the wave propagates, its amplitude decreases as $\delta B \sim r^{-1/2}$ but its relative amplitude increases as $\delta B/B_{\text{bg}} \sim r^{1/2}$. This configuration is qualitatively similar to the propagation of a spherical wave in the magnetosphere of a neutron star, with the exception that $\delta B/B_{\text{bg}}$ increases much more slowly (as $r^{1/2}$ instead of r^2). This modification allows the magnetization $\sigma = B^2/4\pi n_{\pm} m_e c^2$ to decrease much slower with radius, enabling us to cover a larger range of radii r in a single numerical simulation where $\sigma \gg 1$.

We carry out the simulations in 2D polar coordinates using our open source GPU-accelerated PIC code *Aperture*¹. We are primarily interested in the radial evo-

lution of the wave, therefore we simulate only a thin wedge in the θ direction, employing periodic boundary condition on both sides of the wedge. Since the width of the wedge is much smaller than a wavelength, this setup is quasi-1D, without resolving the physics in the transverse direction. The outer radial boundary at r_{out} is set to be open and allows the wave to freely escape. In practice, we usually terminate the simulation before the wave reaches the outer boundary, therefore the outer boundary condition does not affect the results presented below. The box is initially filled with a cold e^{\pm} pair plasma, with $\omega_B \gg \omega_p$, where $\omega_B = eB/m_e c$ is the electron cyclotron frequency and $\omega_p = \sqrt{4\pi n_e e^2/m_e}$ is the plasma frequency. This condition can also be written as $\sigma \gg 1$, where $\sigma = B^2/(4\pi n m_e c^2) = (\omega_B/\omega_p)^2$ is the cold plasma magnetization. The initial temperature of the plasma is $\Theta = kT/m_e c^2 \sim 10^{-2}$, therefore does not contribute significantly to the plasma enthalpy. In order to resolve the gyroradius $\rho_e = m_e c^2/(eB_0)$ of the background magnetic field, we use a uniform grid with 196,608 cells in r and 16 cells in θ . The resolution allows us to maintain $\sigma \gtrsim 10^3$ throughout the simulation domain. We use at least 100 particles per cell per species in our production runs. The simulations were carried out on the OLCF supercomputer *Summit*.

The pair density in the box is chosen to scale as $n_{\pm} \propto r^{-1}$. As a result, ω_p^2/ω_B is a constant throughout the simulation domain. This is motivated by the magnetosphere of a neutron star, where $n_{\pm} \sim r^{-3}$ similar to the dipole magnetic field, assuming the pair multiplicity does not vary appreciably in the magnetosphere. In that case, ω_p^2/ω_B is also a constant throughout the simulation domain. The plasma is initialized with a Maxwellian distribution. The Debye length of this background plasma is larger than the typical gyroradius, thus it is well resolved. Throughout the simulation domain, the magne-

¹ <https://fizban007.github.com/Aperture4.git>

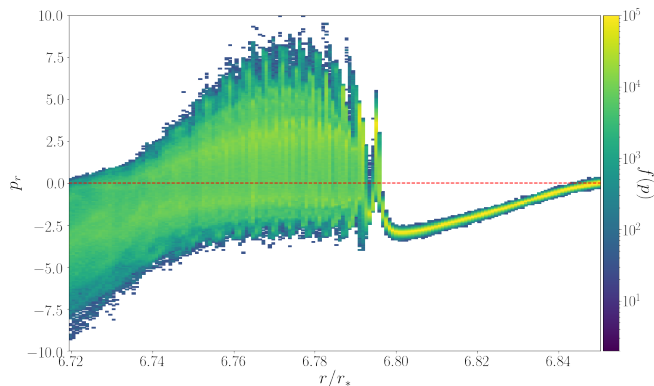


Figure 2. Phase space structure of the first shock in the wave train in the lab frame. The upstream is cold and drifts towards the shock front due to negative $(\mathbf{E} \times \mathbf{B})_r$. The phase space stream forms a solitonic structure as it encounters the shock and oscillates for a few cycles, eventually crossing itself and thermalizing to a temperature $kT_2 \sim \gamma_1 m_e c^2$. This hot plasma proceeds to become the upstream of the subsequent shock.

tization scales as $\sigma \sim r^{-1}$, and the plasma frequency scales as $\omega_p \sim r^{-1/2}$. We ensure that $\omega_p > \omega$ in the whole computational domain, even at the outer edge.

3.2. Results

We performed a series of numerical simulations which can be broadly categorized into two qualitatively different regimes: either the wave nonlinearly steepens into a shock, or $E > B$ regions develop and the wave does not steepen appreciably. Figure 1 shows the result of two simulations with the same parameters except ω_p . For a larger plasma frequency, the waveform deforms to avoid $E > B$ regions (see lower right panel of Figure 1). As a result, the corresponding peak shifts and flattens, leading to a shock that forms behind the deformed wave. In the upstream of this shock, the plasma drifts with $v_r < 0$ into the shock at mildly relativistic speeds, and starts to gyrate in the higher magnetic field in the downstream. In this region ahead of the shock, the plasma drift velocity in the lab frame is always opposite to the wave propagation direction since the total magnetic field B is dominated by the background field B_{bg} , which has opposite sign as the wave magnetic field δB . This stream initially forms a solitonic structure in the phase space, similar to what was originally described by [Alsop & Arons \(1988\)](#) and commonly seen in numerical simulations of perpendicular collisionless shocks (e.g. [Gallant et al. 1992](#); [Plotnikov & Sironi 2019](#)). Eventually the stream self-crosses in the phase space and becomes thermalized, with temperature kT comparable to the drift kinetic energy of the upstream $\gamma_1 m_e c^2$ (Figure 2).

Contrary to [Plotnikov & Sironi \(2019\)](#), we do not observe a notable amount of precursor waves generated

at the shock front, even at the first shock where the upstream plasma is cold. We believe this is due to the high magnetization values in our simulations ($\sigma \gtrsim 10^3$), and the efficiency of generating the precursor wave scales as σ^{-1} ([Plotnikov & Sironi 2019](#); [Sironi et al. 2021](#)). On the other hand, we do see a significant amount of plasma oscillations post-shock, which is evident in the right panels of Figure 1. The power spectrum of the wave before and after it passes through the nonlinear radius is shown in Figure 3. A fraction of the wave energy is deposited to higher frequency modes as a power law, up to the electron gyrofrequency.

On the other hand, for a smaller ω_p , the inertia of the plasma is not sufficient to alter the waveform, leading to E growing larger than B (see upper right panel of Figure 1). The $E > B$ region act as a linear accelerator, accelerating particles to much higher Lorentz factors than the other case. As a result, the plasma becomes only marginally magnetized, with $\omega_B/\gamma \gtrsim \omega$. This prevents subsequent wavelengths to develop a shock as well. The later $E > B$ regions further accelerate the particles. In Section 4, we will discuss semi-analytically the criterion for the two different regimes and compare with the results presented here.

4. CRITERION FOR SHOCK DEVELOPMENT

We aim to derive a criterion for the two qualitatively different regimes presented in Section 3.2. The change of wave electric field is the result of a strong plasma current that is perpendicular to the background magnetic field. In non-relativistic MHD this current takes the general

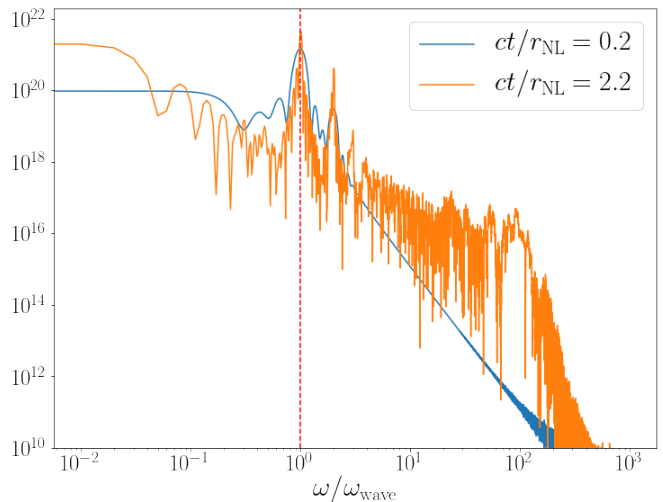


Figure 3. Power spectrum of the electric field before and after the wave passes through the nonlinear radius r_{NL} in the high ω_p case. Red dashed vertical line denotes the frequency of the fms wave. A fraction of the wave energy is converted to high frequency components close to the electron gyrofrequency. The data is taken from the run depicted in the lower right panel of Figure 1.

form:

$$\mathbf{j}_\perp = \frac{\mathbf{B} \times \nabla P}{B^2} + \rho_e \frac{\mathbf{E} \times \mathbf{B}}{B^2} + \rho \frac{\mathbf{B}}{B^2} \times \frac{d\mathbf{v}}{dt}, \quad (5)$$

where \mathbf{v} is the fluid bulk velocity, P is pressure, ρ_e is charge density, and ρ is the mass density. The first term is subdominant in the high σ limit, and the second term is perpendicular to the wave electric field. The third term proportional to $d\mathbf{v}/dt$ is the polarization current, which accounts for the inertia of the plasma. In the relativistic regime, this generalizes to

$$\mathbf{j}_\perp = \frac{\mathbf{B} \times \nabla P}{B^2} + \rho_e \frac{\mathbf{E} \times \mathbf{B}}{B^2} + (\rho_0 + u + P)\gamma^2 \frac{\mathbf{B}}{B^2} \times \frac{d\mathbf{v}}{dt} + \frac{\mathbf{B}}{B^2} \times \mathbf{v} \left(\frac{\partial P}{\partial t} + \mathbf{j} \cdot \mathbf{E} \right), \quad (6)$$

where ρ_0 and u are the rest mass energy density and thermal energy density in the fluid comoving frame, respectively, γ is the bulk Lorentz factor, and $d/dt = \partial/\partial t + \mathbf{v} \cdot \nabla$. When the fluid Lorentz factor becomes significant, \mathbf{j}_\perp is dominated by the polarization current proportional to γ^2 , which is along the \mathbf{E} field direction. This is the current that changes the wave form and ultimately causes the shock to develop.

Consider the cylindrical wave in the numerical simulations of Section 3.2. The perpendicular current is along the z direction. For a small amplitude fms wave in the high magnetization regime, this current is typically very small compared to the displacement current, $j_z/(\nabla \times \mathbf{B}) \sim 1/\sigma$, and it vanishes in the force-free limit since the rest mass energy density goes to zero. However, as $\delta B/B_{\text{bg}}$ approaches $1/2$, this current increases significantly, up to $j_z \sim 0.1n_\pm ec$ as we measured empirically in our simulations. This is the maximum rate at which the wave field δE can change compared to its force-free counterpart.

On the other hand, the background magnetic field changes on a completely independent time scale which is set by the global structure of the magnetosphere. The magnetic field of an infinite cylinder drops as $B_{\text{bg}} \sim r^{-1}$, while the wave field δE naturally drops as $\delta E \sim r^{-1/2}$. In order to avoid $E > B$ regions in the wave, the plasma current j_\perp needs to reduce the wave field such that it decreases at least as fast as the background field. Consider the wave propagating from some radius r_0 to $r_0 + \Delta r$ during time $\Delta t \approx \Delta r/c$, the criterion for avoiding $E > B$ becomes:

$$4\pi j_\perp \Delta t \gtrsim \delta E \left[\left(1 + \frac{\Delta r}{r_0} \right)^{-1/2} - \left(1 + \frac{\Delta r}{r_0} \right)^{-1} \right] \quad (7)$$

$$\approx \delta E \frac{1}{2} \frac{\Delta r}{r_0}.$$

If we evaluate this equation near the nonlinear radius, where $\delta E = \delta B \sim B_{\text{bg}}/2$, and use $j_\perp \sim 0.1n_\pm ec$, we can

write down the criterion for forming a shock at r_{NL} :

$$0.1\omega_p^2 \gtrsim \frac{1}{2} \frac{c}{r_{\text{NL}}} \frac{\omega_B}{2}, \quad (8)$$

where $\omega_B = eB_{\text{bg}}/m_e c$ is the gyrofrequency in the background magnetic field. Note that the coefficient of $1/2$ depends on the geometry, and becomes 2 for spherical waves propagating in a dipole magnetic field. Therefore, a crude criterion for the formation of collisionless shocks at each wavelength when the fms wave comes near the nonlinear radius is:

$$\eta \equiv \frac{\omega_p^2 r_{\text{NL}}}{c\omega_B} \gtrsim \begin{cases} 2.5, & \text{if } \delta B/B_{\text{bg}} \sim r^{1/2}, \\ 10, & \text{if } \delta B/B_{\text{bg}} \sim r^2. \end{cases} \quad (9)$$

The right panel of Figure 1 shows two contrasting simulations with the dimensionless ratio η below and above the threshold, and we see indeed that in the latter case shocks are formed in the wave and no $E > B$ regions are developed.

Taking this approximate criterion for development of shocks, we are interested in whether typical FRBs produced in the inner magnetosphere will develop shocks near the nonlinear radius, or propagate as vacuum waves as suggested by Beloborodov (2021). For typical FRB parameters estimated in Section 2, this ratio η can be evaluated as:

$$\eta = \frac{\omega_p^2 r_{\text{NL}}}{c\omega_B} \sim 7.8 \times 10^4 B_{0,14}^{-1/2} L_{\text{wave},42}^{-1/4} L_{\text{keV},35}. \quad (10)$$

This is much larger than the threshold value of ~ 10 for a dipole background field, therefore we expect typical cosmological FRBs produced in the magnetospheres of magnetars to steepen into shocks easily when they become nonlinear due to propagation.

Since this dimensionless ratio does not depend on the frequency of the fms wave (as long as $\omega_p \gg \omega$), the same conclusion applies to low frequency kHz fast waves launched directly from the magnetar either due to star quakes, or due to nonlinear conversion from Alfvén waves (Yuan et al. 2021). A kHz fms wave with isotropic equivalent luminosity in a wide luminosity range of 10^{36} erg/s to 10^{42} erg/s will inevitably steepen into shocks within the magnetosphere. This mechanism can serve as an alternative way to launch shocks from the magnetosphere of a magnetar, without the need for a relativistic ejecta such as proposed by Yuan et al. (2020, 2022). Formation of the shock may shift a fraction of the wave energy into high frequency components, as shown in Section 3.2. Eventually, the shock may also become an efficient emitter of coherent radio waves when it propagates to large distances from the star through the synchrotron maser mechanism (Plotnikov & Sironi 2019; Sironi et al. 2021).

5. WAVE DISSIPATION THROUGH SHOCKS

In the highly magnetized limit where collisionless perpendicular shocks do form, dissipation of the fast wave is mainly mediated through these shocks. We seek to describe this dissipation process and evaluate how quickly waves of different wavelengths will lose their energy through this mechanism.

Plasma heating through perpendicular shocks has been well-studied theoretically (see e.g. Gallant et al. 1992; Amato & Arons 2006). A synchrotron maser forms at the front of the shock, coherently reflecting particles from the upstream and thermalizing their bulk motion (Hoshino & Arons 1991; Gallant et al. 1992). By writing down the shock jump condition in the downstream rest frame, one can find the heating of the downstream as a function of the upstream Lorentz factor and magnetization σ , and the adiabatic index Γ . For a cold upstream, Gallant et al. (1992) found that for e^\pm plasma in the high σ limit:

$$\frac{kT_2}{\gamma_{12}m_e c^2} = \frac{2(\Gamma - 1)}{4 - \Gamma} + \frac{2\Gamma(\Gamma - 1)(2 - \Gamma)}{(4 - \Gamma)^3} \frac{1}{\sigma} + O\left(\frac{1}{\sigma^2}\right), \quad (11)$$

where γ_{12} is the upstream bulk Lorentz factor measured in the downstream frame. The plasma moves in the plane perpendicular to the background magnetic field, therefore it is appropriate to use an adiabatic index of $\Gamma \rightarrow 3/2$.

In the case of an fms wave train described in this paper, a relativistic perpendicular shock may form at every wavelength. Only the first shock in the wave train may encounter a cold upstream, whereas every subsequent shock will encounter the heated downstream of the preceding shock. In order to predict the total dissipation power and plasma heating, we need the generalization of Equation (11) in the case of a finite upstream temperature. For pedagogical reasons we include a derivation in Appendix A, where we write down the shock jump condition in the shock rest frame, then use it to derive a constraint on shock heating:

$$\frac{T_2}{T_1} \lesssim 1.7\gamma_1 \left(1 + \frac{0.32}{\sigma} + O(\sigma^{-2})\right), \quad (12)$$

where T_1 and T_2 are the upstream and downstream plasma temperatures measured in the respective comoving frame, γ_1 is the upstream bulk Lorentz factor measured in the lab frame, and σ is the upstream magnetization. Across every shock except the first, the downstream is heated with respect to the upstream by a factor of $\sim\gamma_1$. In the case of a constant γ_1 , the plasma temperature increases *exponentially* across many consecutive shocks. In our simulations, the upstream Lorentz factor γ_1 remains at most mildly relativistic, especially when η is far above the threshold [Equation (9)] and the shock is easily formed.

This exponential heating cannot continue indefinitely as the wave will soon deplete its energy. Several phys-

ical mechanisms will kick in before the wave energy is depleted. The shock heating will become inefficient when the plasma is heated to a high enough temperature such that the gyroradius of the hot electrons become comparable to the wavelength of the fms wave, $kT/m_e c^2 \sim \omega_B/\omega$. Near the nonlinear radius r_{NL} this temperature will be:

$$\Theta_{\text{demag}} \sim \frac{\omega_B}{\omega} \sim 8.0 \times 10^5 B_{0,14}^{-1/2} L_{\text{wave},42}^{3/4}. \quad (13)$$

At this temperature, the plasma becomes essentially demagnetized and collisionless shocks will not form within a wavelength anymore.

Another mechanism that will limit plasma heating is the radiative cooling of the downstream through synchrotron emission. Within the magnetar magnetosphere where the background magnetic field is high, synchrotron cooling can place a strong limit on the temperature of the plasma. This limit can be estimated by equating the heating rate with the synchrotron cooling rate:

$$\frac{kT_2 - kT_1}{\omega^{-1}} \sim \frac{4}{3} \left(\frac{kT_2}{m_e c^2}\right)^2 \sigma_T c U_B. \quad (14)$$

Using $T_2 \sim 1.7\gamma_1 T_1$ and assuming $\gamma_1 \sim 2$, the upstream temperature at which shock heating balances synchrotron cooling becomes:

$$\Theta_1 \equiv \frac{kT_1}{m_e c^2} \sim \frac{1}{6.4\ell_\lambda}, \quad (15)$$

where ℓ_λ can be understood as the magnetic compactness over an fms wavelength: $\ell_\lambda \equiv \sigma_T U_B \lambda / m_e c^2$. At this temperature, subsequent shocks passing through the plasma will dissipate at a steady rate:

$$\dot{U} \sim \omega k(T_2 - T_1)n_\pm \sim 0.37 \frac{\omega n_\pm m_e c^2}{\ell_\lambda}. \quad (16)$$

All the energy dissipated in the shock is radiated away through synchrotron radiation.

We can estimate the dissipation time scale for an FRB-like fms wave propagating in the closed magnetic field line zone of the magnetar. Taking the estimates for r_{NL} in Section 2, the magnetic compactness ℓ_λ over the wavelength of a GHz FRB is:

$$\ell_\lambda = 2.0 \times 10^{-3} \left(\frac{r}{r_{\text{NL}}}\right)^{-6} B_{0,14}^{-1} L_{\text{wave},42}^{3/2}. \quad (17)$$

The compactness decreases rapidly with increasing radius. As a result, the synchrotron balanced temperature is $\Theta_1 \sim 10^2$ near the nonlinear radius, and grows as r^6 . The dissipation rate \dot{U} is proportional to n_\pm/ℓ_λ , which scales as r^3 . Due to the nature of exponential heating over consecutive shocks, $\Theta_1 \sim 10^2$ can be reached very quickly after only a few wavelengths. A typical 1 ms FRB contains 10^6 wavelengths, thus all but the

first few wavelengths will pass through a hot plasma at this radiation-balanced temperature.

Near the nonlinear radius, the total dissipation power of an FRB assuming isotropic emission is:

$$L_{\text{diss}} \sim 4\pi r_{\text{NL}}^2 c \Delta t \dot{U} \sim 4.4 \times 10^{42} \text{ erg/s}, \quad (18)$$

where Δt is the duration of the burst. This high dissipation power means that a significant fraction of the FRB energy will be converted to radiation within the duration of the FRB itself. The resulting radiation will have an energy of a few keV, and the $\Theta \sim 100$ plasma upscattering this soft X-ray will produce ~ 10 MeV soft γ -rays which can convert into e^\pm pairs. The total magnetic compactness of the FRB wave train can be very high, $\ell_B \gtrsim 10^3$, and we expect significant pair loading at the nonlinear radius where the FRB is dissipated. A detailed calculation of the pair loading and subsequent radiation signature is beyond the scope of the current paper, and will be studied in a future work. Effectively, the FRB will likely not be able to escape the magnetosphere.

For a kHz fms wave launched near the magnetar surface, the wavelength is much larger and there are fewer shocks in total for the same duration. As a result, the magnetic compactness per wavelength ℓ_λ is significantly higher, $\ell_\lambda \sim 10^3$. Equation (15) predicts a temperature much lower than unity, suggesting that the plasma has plenty of time to cool to nonrelativistic temperatures before encountering a second shock. It is therefore a good approximation to treat each shock as propagating into a cold upstream, and we expect only mild heating of the plasma from these shocks in the high σ region in the magnetar magnetosphere, instead of the exponential growth of the plasma temperature in the case with no cooling. The exact heating rate is given by Equation (11) and depends critically on the upstream Lorentz factor γ_1 . More study is required to quantify its dependence on the plasma properties such as magnetization σ , gradient of the background magnetic field, and plasma frequency ω_p . Due to high magnetic compactness in this region, synchrotron radiation may interact nontrivially with the plasma in the shock. This topic is again out of the scope of the current paper, but is worth looking into analytically or through PIC simulations in the future.

6. DISCUSSIONS

We have studied the propagation of a strong fast magnetosonic (fms) wave across a slowly decreasing background magnetic field. The wave may become nonlinear, in other words $|\delta\mathbf{E}| \gtrsim |\delta\mathbf{B} + \mathbf{B}_{\text{bg}}|$, as a result of propagation. We found that when the plasma is well magnetized, its collective response is important when the wave becomes nonlinear, and collisionless perpendicular shocks may self-consistently develop at every wavelength as a result. We derived a simple analytic criterion [Equation (9)] for when shocks will develop, and concluded

that these shocks will form for most cosmological FRBs as well as low frequency kHz fast waves from the star. As a result of these shocks, FRBs produced deep within the magnetosphere propagating in the closed field line zone may dissipate completely within 1 ms when it becomes nonlinear, converting its energy into e^\pm pairs and high energy radiation. Low frequency kHz fast waves do not suffer as much dissipation, but may form strong perpendicular shocks that can propagate to large distances and produce FRBs through the synchrotron maser mechanism.

One crucial simplification of the simulations presented in Section 3 was that we considered the global magnetic field of a current-carrying cylinder rather than a spherical star with dipole magnetic field. As a result, we have $\delta B/B_{\text{bg}} \sim r^{1/2}$ instead of the realistic case where $\delta B/B_{\text{bg}} \sim r^2$. Most notably, the relative strength of the wave grows slower at large radii in the cylindrical case, while it grows faster and faster in a dipole magnetosphere. This difference may have implications on the long term behavior of the shocks formed near r_{NL} , and should be studied in the future using global PIC simulations in spherical coordinates.

Despite our usage of PIC simulations to study this problem, the magnetized regime where shocks form can be well-described by relativistic MHD. An analytic model based on MHD equations, similar to what was developed by Lyubarsky (2003), can give better estimates on the upstream Lorentz factors γ_1 at each shock. Such a calculation will improve the estimates of shock heating and provide better constraints on the wave dissipation rate. More systematic PIC simulations of the shocks at a variety of parameter regimes will also allow us to better understand the transition from the well-magnetized MHD regime to the vacuum-like regime, and potentially test the wave scattering theory proposed by Beloborodov (2022).

Radiative effects and pair production at the shocks are also interesting by-products in these low frequency fast waves when they become nonlinear. As estimated in Section 5, an FRB dissipated through this mechanism may lead to strong pair loading and an X-ray flare. Future works in this direction can potentially lead to better theoretical understanding of the rich X-ray phenomenology concerning magnetars.

ACKNOWLEDGMENTS

We thank Yuri Levin, Andrei Beloborodov, Dmitri Uzdensky, and Greg Werner for helpful discussions. AC acknowledges support from Fermi Guest Investigation grant 80NSSC21K2027. AC and YY acknowledge support from NSF grant DMS-2235457. XL is supported by NSERC, funding reference #CITA 490888-16 and the Jeffrey L. Bishop Fellowship. This work was also

facilitated by Multimessenger Plasma Physics Center (MPPC), NSF grant PHY-2206608. This research used resources of the Oak Ridge Leadership Computing Facil-

ity at the Oak Ridge National Laboratory, which is supported by the Office of Science of the U.S. Department of Energy under Contract No. DE-AC05-00OR22725.

APPENDIX

A. SHOCK JUMP CONDITION FOR A MAGNETIZED RELATIVISTIC FLUID

For a magnetized relativistic fluid, its stress-energy tensor is given by

$$T^{\mu\nu} = \left(\rho h + \frac{b^2}{4\pi}\right) u^\mu u^\nu + \left(P + \frac{b^2}{8\pi}\right) g^{\mu\nu} - \frac{b^\mu b^\nu}{4\pi}. \quad (\text{A1})$$

Here g is metric tensor, h is specific enthalpy, P is pressure, u is 4-velocity, and $b^\mu = u_\nu F^{*\mu\nu}$ is magnetic field in the comoving frame, $b^2 = b_\mu b^\mu$. All thermodynamical quantities are defined in the comoving frame of the fluid. We consider the fluid as an ideal gas consisting of collisionless particle with equation of state $P = \rho^\Gamma$ and specific internal energy dominated by relativistic thermal motion. Therefore $h = \kappa P/\rho$ is proportional to the fluid temperature T and $\kappa = \Gamma/(\Gamma - 1)$.

The fluid evolves under the conservation laws of matter and stress-energy, plus the Maxwell equations.

$$\nabla_\mu(\rho u^\mu) = 0 \quad (\text{A2})$$

$$\nabla_\mu T^{\mu\nu} = 0 \quad (\text{A3})$$

$$\nabla_\mu F^{*\mu\nu} = 0. \quad (\text{A4})$$

For the shock in 1D with perpendicular magnetic field, we can reach the following shock jump condition in the shock frame

$$[[\rho\gamma\beta]] = 0 \quad (\text{A5})$$

$$[[b\gamma\beta]] = 0 \quad (\text{A6})$$

$$\left[\left(\rho h + \frac{b^2}{4\pi} \right) \gamma^2 \beta \right] = 0 \quad (\text{A7})$$

$$\left[\left(\rho h + \frac{b^2}{4\pi} \right) \gamma^2 \beta^2 + \frac{b^2}{8\pi} + P \right] = 0. \quad (\text{A8})$$

Here we define the operator $[[Q]] = Q_1 - Q_2$, is the difference of quantity Q across the shock with the subscript 1 standing for upstream and 2 for downstream. Introducing the velocity ratio $r \equiv \beta_2/\beta_1$, we have

$$\frac{\gamma_2}{\gamma_1} = \sqrt{\frac{1 - \beta_1^2}{1 - r^2 \beta_1^2}}. \quad (\text{A9})$$

$$\frac{\rho_2}{\rho_1} = \frac{b_2}{b_1} = \frac{\gamma_1 \beta_1}{\gamma_2 \beta_2} = \frac{1}{r} \sqrt{\frac{1 - r^2 \beta_1^2}{1 - \beta_1^2}}. \quad (\text{A10})$$

From Equation A7, the energy ratio and enthalpy ratio across the shock is

$$\frac{\rho_2 h_2 + b_2^2/4\pi}{\rho_1 h_1 + b_1^2/4\pi} = \frac{\gamma_1^2 \beta_1}{\gamma_2^2 \beta_2} \quad (\text{A11})$$

$$\frac{h_2}{h_1} = \frac{\gamma_1}{\gamma_2} + \sigma_1 \frac{\gamma_1}{\gamma_2} \left(1 - \frac{1}{r} \right) \quad (\text{A12})$$

where $\sigma = b^2/4\pi\rho h$ is the hot plasma magnetization.

Using Equation A8 we obtain an equation for r

$$(r - 1) \left[\left(1 - \frac{1}{\kappa} \right) (1 + \sigma_1) \beta_1^2 r^2 - \left(\frac{1}{\kappa} + \frac{\sigma_1}{2} \right) r + \sigma_1 \left(\frac{1}{\kappa} - \frac{1}{2} \right) \right] = 0 \quad (\text{A13})$$

which admits a nontrivial solution

$$r = \frac{2 + \kappa\sigma_1 + \sqrt{(2 + \kappa\sigma_1)^2 + 8\beta_1^2(\kappa - 1)(\kappa - 2)\sigma_1(\sigma_1 + 1)}}{2\beta_1^2(\kappa - 1)(\sigma_1 + 1)}. \quad (\text{A14})$$

For physical conditions where the shock compresses the fluid, $r < 1$

$$\beta_1 > \sqrt{\frac{\Gamma - 1 + \sigma_1}{1 + \sigma_1}} = \frac{\Gamma P + b^2/4\pi}{\rho h + b^2/4\pi} = \beta_F \quad (\text{A15})$$

where β_F is the ratio of the fast magnetosonic speed over the speed of light. The upstream fluid must move supersonically to trigger the shock.

The (comoving) temperature of the fluid is given by $T \propto P/\rho \propto h$, therefore the shock will heat the fluid by

$$\frac{T_2}{T_1} = \frac{\gamma_1}{\gamma_2} \left(1 + \sigma_1 - \frac{\sigma_1}{r}\right). \quad (\text{A16})$$

Assuming that the shock moves at the speed $\beta_{\text{sh}}c$, we can express the temperature ratio in terms of the lab frame bulk Lorentz factors $\tilde{\gamma}_1$ and $\tilde{\gamma}_2$

$$\frac{T_2}{T_1} = \frac{\tilde{\gamma}_1 + \beta_{\text{sh}}\sqrt{\tilde{\gamma}_1^2 - 1}}{\tilde{\gamma}_2 - \beta_{\text{sh}}\sqrt{\tilde{\gamma}_2^2 - 1}} \left(1 + \sigma_1 - \frac{\sigma_1}{r}\right). \quad (\text{A17})$$

We specialize to a 2D relativistic plasma where $\Gamma = 3/2$ and $\kappa = 3$. In the limit of an ultra-relativistic fluid, $\beta_1 \rightarrow 1$, and high upstream magnetization, $\sigma_1 \rightarrow \infty$, we have

$$r = 1 - \frac{2}{5\sigma_1} + \frac{44}{125\sigma_1^2} + \mathcal{O}(\sigma_1^{-3}) \quad (\text{A18})$$

and

$$\frac{T_2}{T_1} = \frac{\tilde{\gamma}_1 + \beta_{\text{sh}}\sqrt{\tilde{\gamma}_1^2 - 1}}{\tilde{\gamma}_2 - \beta_{\text{sh}}\sqrt{\tilde{\gamma}_2^2 - 1}} \left(\frac{3}{5} + \frac{24}{125\sigma_1} + \mathcal{O}(\sigma_1^{-2})\right). \quad (\text{A19})$$

In the context of perpendicular shocks launched by the nonlinear steepening of fast magnetosonic waves described in Section 3, the values of $\tilde{\gamma}_1$ and $\tilde{\gamma}_2$ are given by the upstream and downstream electromagnetic fields. In the downstream, $B = B_{\text{bg}} + \delta B$ where $\delta B \lesssim B_{\text{bg}}/2$, and the fluid bulk velocity is simply given by the $\mathbf{E} \times \mathbf{B}$ drift: $\tilde{v}_2 \sim \delta E/B \lesssim 1/3$ and $\tilde{\gamma}_2 \lesssim 1.06$. Since $\beta_{\text{sh}} < 1$ by construction, we can estimate the shock heating rate:

$$\frac{T_2}{T_1} \lesssim 1.7\tilde{\gamma}_1 \left(1 + \frac{0.32}{\sigma_1} + \mathcal{O}(\sigma_1^{-2})\right) \quad (\text{A20})$$

REFERENCES

- Alsop, D., & Arons, J. 1988, *Physics of Fluids*, 31, 839, doi: [10.1063/1.866765](https://doi.org/10.1063/1.866765)
- Amato, E., & Arons, J. 2006, *ApJ*, 653, 325, doi: [10.1086/508050](https://doi.org/10.1086/508050)
- Arons, J., & Barnard, J. J. 1986, *ApJ*, 302, 120, doi: [10.1086/163978](https://doi.org/10.1086/163978)
- Beloborodov, A. M. 2021, *ApJL*, 922, L7, doi: [10.3847/2041-8213/ac2fa0](https://doi.org/10.3847/2041-8213/ac2fa0)
- . 2022, *PhRvL*, 128, 255003, doi: [10.1103/PhysRevLett.128.255003](https://doi.org/10.1103/PhysRevLett.128.255003)
- Blaes, O., Blandford, R., Goldreich, P., & Madau, P. 1989, *ApJ*, 343, 839, doi: [10.1086/167754](https://doi.org/10.1086/167754)
- Bochenek, C. D., Ravi, V., Belov, K. V., et al. 2020, *Nature*, 587, 59, doi: [10.1038/s41586-020-2872-x](https://doi.org/10.1038/s41586-020-2872-x)
- Bransgrove, A., Beloborodov, A. M., & Levin, Y. 2020, *ApJ*, 897, 173, doi: [10.3847/1538-4357/ab93b7](https://doi.org/10.3847/1538-4357/ab93b7)
- CHIME/FRB Collaboration, Andersen, B. C., Bandura, K. M., et al. 2020, *Nature*, 587, 54, doi: [10.1038/s41586-020-2863-y](https://doi.org/10.1038/s41586-020-2863-y)
- Gallant, Y. A., Hoshino, M., Langdon, A. B., Arons, J., & Max, C. E. 1992, *ApJ*, 391, 73, doi: [10.1086/171326](https://doi.org/10.1086/171326)
- Hoshino, M., & Arons, J. 1991, *Physics of Fluids B*, 3, 818, doi: [10.1063/1.859877](https://doi.org/10.1063/1.859877)
- Kumar, P., Lu, W., & Bhattacharya, M. 2017, *MNRAS*, 468, 2726, doi: [10.1093/mnras/stx665](https://doi.org/10.1093/mnras/stx665)

- Li, X., Zrake, J., & Beloborodov, A. M. 2019, *ApJ*, 881, 13, doi: [10.3847/1538-4357/ab2a03](https://doi.org/10.3847/1538-4357/ab2a03)
- Lu, W., Kumar, P., & Zhang, B. 2020, *MNRAS*, 498, 1397, doi: [10.1093/mnras/staa2450](https://doi.org/10.1093/mnras/staa2450)
- Lyubarsky, Y. 2014, *MNRAS*, 442, L9, doi: [10.1093/mnrasl/slu046](https://doi.org/10.1093/mnrasl/slu046)
- . 2020, *ApJ*, 897, 1, doi: [10.3847/1538-4357/ab97b5](https://doi.org/10.3847/1538-4357/ab97b5)
- Lyubarsky, Y. E. 2003, *MNRAS*, 339, 765, doi: [10.1046/j.1365-8711.2003.06221.x](https://doi.org/10.1046/j.1365-8711.2003.06221.x)
- Mereghetti, S., Savchenko, V., Ferrigno, C., et al. 2020, *ApJL*, 898, L29, doi: [10.3847/2041-8213/aba2cf](https://doi.org/10.3847/2041-8213/aba2cf)
- Petroff, E., Hessels, J. W. T., & Lorimer, D. R. 2019, *A&A Rv*, 27, 4, doi: [10.1007/s00159-019-0116-6](https://doi.org/10.1007/s00159-019-0116-6)
- Plotnikov, I., & Sironi, L. 2019, *MNRAS*, 485, 3816, doi: [10.1093/mnras/stz640](https://doi.org/10.1093/mnras/stz640)
- Qu, Y., Kumar, P., & Zhang, B. 2022, *MNRAS*, 515, 2020, doi: [10.1093/mnras/stac1910](https://doi.org/10.1093/mnras/stac1910)
- Sironi, L., Plotnikov, I., Nättilä, J., & Beloborodov, A. M. 2021, *PhRvL*, 127, 035101, doi: [10.1103/PhysRevLett.127.035101](https://doi.org/10.1103/PhysRevLett.127.035101)
- Thompson, C., & Duncan, R. C. 1996, *ApJ*, 473, 322, doi: [10.1086/178147](https://doi.org/10.1086/178147)
- Yuan, Y., Beloborodov, A. M., Chen, A. Y., & Levin, Y. 2020, *ApJL*, 900, L21, doi: [10.3847/2041-8213/abafa8](https://doi.org/10.3847/2041-8213/abafa8)
- Yuan, Y., Beloborodov, A. M., Chen, A. Y., et al. 2022, *ApJ*, 933, 174, doi: [10.3847/1538-4357/ac7529](https://doi.org/10.3847/1538-4357/ac7529)
- Yuan, Y., Levin, Y., Bransgrove, A., & Philippov, A. 2021, *ApJ*, 908, 176, doi: [10.3847/1538-4357/abd405](https://doi.org/10.3847/1538-4357/abd405)